



Associated conference: 5th International Small Sample Test Techniques Conference

Conference location: Swansea University, Bay Campus

Conference date: 10th - 12 July 2018

How to cite: Altstadt, E., Houska, M. & Das, A. 2018. Effect of anisotropic microstructure of ODS steels on small punch test results. *Ubiquity Proceedings*, 1(S1): 4 DOI: <https://doi.org/10.5334/uproc.4>

Published on: 10 September 2018

Copyright: © 2018 The Author(s). This is an open-access article distributed under the terms of the Creative Commons Attribution 4.0 International License (CC-BY 4.0), which permits unrestricted use, distribution, and reproduction in any medium, provided the original author and source are credited. See <http://creativecommons.org/licenses/by/4.0/>.

UBIQUITY PROCEEDINGS



<https://ubiquityproceedings.com>

Effect of anisotropic microstructure of ODS steels on small punch test results

E. Altstadt^{1,*}, M. Houska² and A. Das³

¹ Helmholtz-Zentrum Dresden-Rossendorf, Germany; e.altstadt@hzdr.de

² Helmholtz-Zentrum Dresden-Rossendorf, Germany; m.houska@hzdr.de

³ Helmholtz-Zentrum Dresden-Rossendorf, Germany; a.das@hzdr.de

* Correspondence: e.altstadt@hzdr.de; Tel.: +49-351-260-2276

Abstract: Oxide dispersed strengthened (ODS) steels can exhibit a strongly anisotropic microstructure leading to anisotropic mechanical properties. The ductile to brittle transition temperature in the small punch (SP) test is therefore dependent on the specimen orientation. Three ODS steels with 13-14 mass percent Cr, manufactured through hot extrusion and hot rolling respectively, were investigated by means of SPT in different orientations. Existing microstructural data (EBSD) are used to discuss the anisotropic fracture behavior observed in the SPT. In addition, the SPT results are compared with those from existing fracture mechanics tests based on sub-sized C(T) samples. The applicability of the empirical conversion of SPT based transition temperatures into Charpy transition temperatures – well established for isotropic homogeneous metals – is investigated for materials with anisotropic microstructure.

Keywords: small punch test, ductile-to-brittle transition temperature, oxide dispersion strengthened steel

1. Introduction

Oxide dispersion strengthened (ODS) steels are candidate materials for fuel claddings of Gen-IV sodium cooled fast reactors as well as for the first wall and blanket structures of fusion reactors [1–3]. The envisaged operation temperature is up to 650 °C. The focus of ODS materials development was put on superior creep and swelling properties. However, sufficient tensile and fracture mechanical properties are required for safety relevant structural applications in the whole range from room to operation temperature. Lindau et al. demonstrated that yield stress and ultimate tensile stress (UTS) of ODS-EUROFER are significantly higher in comparison to the non ODS EUROFER steel for temperatures up to 750 °C [4]. The creep resistance at 750 °C is also significantly improved. However, the ductile-to-brittle transition temperature (DBTT) was found to be significantly higher than that of non-ODS-EUROFER. Chaouadi et al. [5] found a significant crack resistance degradation of Eurofer ODS when the test temperature increases. In particular, at 550 °C and 650 °C, the crack resistance is very low. Nevertheless, Byun et al. [6] have demonstrated that high temperature fracture toughness could be significantly improved by appropriate thermo-mechanical treatments.

The fracture behavior of ODS materials is governed by grain morphology. Chao et al. [7] found a grain size anisotropy for a 20Cr ODS alloy manufactured as a tube by hot rolling. The grains were found to be elongated along the rolling direction. KLST impact tests and subsequent EBSD analyses of the crack region revealed intergranular cracks along the elongated grain boundaries which constitute weak interfaces. The term “delamination” originating from laminated composite materials was adopted for this type of intergranular cracking. The delamination phenomenon had earlier been reported for ultrafine grain structure steels by Kimura et al. [8]. Depending on the orientation of the weak planes in the impact specimen, they discriminated a “crack arrester” and a “crack divider” situation. The impact of two different fabrication routes (hot rolling and hot extrusion) on the grain morphology and thereby on the fracture toughness in different orientations was investigated in detail by Das et al. [9,10].

The small punch (SP) test has long been accepted as a method to estimate mechanical properties from small quantities of materials. In particular the ductile to brittle transition temperature, the yield stress, the ultimate tensile stress and creep strength can be extracted for homogeneous and isotropic metals [11–19]. The SP test is not intended to replace conventional tests such as tensile tests, Charpy impact tests or fracture mechanical testing, but to be used as screening procedure [17]. The SP test is especially useful in one or more of the following cases: (i) the available amount of material is limited, (ii) the material is highly activated by neutron irradiation, (iii) material properties are non-homogeneous and exhibit significant gradients. Therefore it is generally useful to include this technique in the characterization of ODS alloys. So far, the effect of the above mentioned anisotropic microstructure on SP test

results has only rarely been investigated [20,21]. A systematic comparison with impact tests and fracture mechanics tests is needed. In this paper we investigate one hot rolled and two hot extruded ODS steels by means of SP testing. The SP results are discussed in the view of existing fracture mechanics tests for the same materials. The paper aims at relating fracture mechanisms depending on grain morphology and orientation to features of SP force-displacement curves and SP based DBTTs.

2. Materials and Methods

Three different ODS steels were selected for testing, one hot-rolled and two hot-extruded. The denomination in this paper is ODS-HR, ODS-HE-1, ODS-HE-2. The bulk chemical composition of the materials is given in Table 1.

- **ODS-HR** is a 13%Cr ODS steel hot rolled plate provided by Karlsruhe Institute of Technology, Germany (KIT). The main production steps include: mechanical alloying in an attritor ball mill, encapsulation of the powder, hot isostatic pressing at 1100 °C and 100 MPa and rolling at 1100 °C from a diameter of 80 mm to a plate of 8 mm thickness in 5 runs [9,22].
- **ODS-HE-1** is a hot extruded 13% Cr ODS steel round bar also provided KIT. The main fabrication steps include: mechanical alloying in an attritor ball mill, encapsulation of the powder, evacuation of the capsule and hot extrusion at 1100 °C [10,22].
- **ODS-HE-2** is a hot extruded 14% Cr ODS steel round bar provided by Centro Sviluppo Materiali, Italy (CSM). Gas atomized pre-alloyed steel powder was mixed with 0.3% Y₂O₃ and dry ball milled in an environment of Ar and H. After canning, direct hot extrusion was performed at 1150 °C with an extrusion ratio of 22.5. A heat treatment at 1050 °C was applied for one hour with subsequent cooling in the furnace [10].

Table 1. Chemical composition of the tested ODS steels (wt%) [9,10,22].

Material	C	Si	P	Ti	Cr	Ni	W	Y ₂ O ₃ *
ODS-HR	0.21	-	-	0.151	13.10	0.09	1.11	0.3
ODS-HE-1	0.028	0.051	0.01	0.138	12.99	0.101	1.03	0.3
ODS-HE-2	0.010	0.371	0.006	0.238	13.76	0.239	0.84	0.3

* Nominal Y₂O₃ content of the powder composition

Small punch tests were executed in three orientations for ODS-HR (S - thickness direction, L - rolling direction and T - transverse direction) and in two orientations for ODS-HE-1 and ODS-HE-2 (L - extrusion direction, R/C - radial/circumferential direction). The orientation refers to the normal direction of the specimens. In case of ODS-HE-1 and ODS-HE-2, it is assumed that the directions R and C are equivalent because of the axial symmetry of the extrusion process. Moreover, plane samples cut from a round bar in axial direction always exhibit a combination of R and C orientation for geometrical reasons. One can assume a plane stress state in a SP test, i.e. the stress components in thickness direction are much smaller than the in-plane stress components. Therefore the S oriented specimens represent the mechanical behavior of the LT plane, the T oriented specimens those of the LS plane and the L oriented specimens those of the TS plane [21].

Specimens of Ø8 x 0.5 mm were manufactured by electrical discharge machining and subsequent grinding to final thickness with grit 2500. The maximum accepted thickness tolerance was ±5 µm. The thicknesses of all specimens were measured by laser micrometer with an accuracy of ±1 µm. Specimens with a thickness outside the tolerance were not used. The main parameters of the SP set-up are: punch diameter $d = 2.5$ mm, receiving hole diameter $D = 4$ mm, receiving hole edge radius $R_E = 0.5$ mm (cf. Fig. 1). The edge size is larger than proposed in the upcoming standard [23]. While the effect of the edge size on the estimation of tensile properties (in particular the yield stress) is significant, it can be neglected for the estimation of the ductile to brittle transition temperature [17].

The punch displacement v was measured by an inductive sensor with an accuracy of ±1 µm and corrected for the device compliance. The punch force was measured by means of a load cell placed between the puncher and the cross head of the testing machine with an accuracy of ±5 N.

In total a number of 168 tests were performed. The temperature range was from -188 °C to +350 °C. The subsequent fractographic analysis of the tested SP specimens was done by SEM using a Zeiss EVO 50 device.

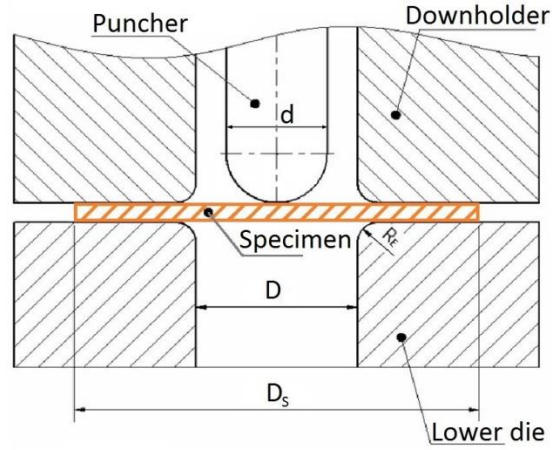


Figure 1. Geometry of the SP set-up.

The SP based ductile-to-brittle transition temperature T_{SP} is determined on the basis of normalized energies $E_n = E_{SP}/F_m$ [24] of the different tests. E_{SP} is the area under the force-displacement curve up to the displacement v_m at maximum force F_m :

$$E_{SP} = \int_0^{v_m} F(v) dv \approx \sum_{k=2}^{k_{\max}} (F_k + F_{k-1})(v_k - v_{k-1}) \quad (1)$$

A tanh-fitting procedure was applied for the $E_n(T)$ dependence based on the following equation:

$$E_n(T) = A + B \cdot \tanh \left[\frac{T - T_{SP}}{C} \right] \quad (2)$$

A least square procedure was used to determine the coefficients A , B , C , and T_{SP} . The Charpy transition temperature T_{CVN} can be recalculated by the well-known correlation $T_{SP} = \alpha T_{CVN}$ (temperatures in K) [14]. For our set-up we used $\alpha = 0.43$ [17]. This value was further validated for a number of ferritic-martensitic steels and reactor pressure vessel steels. However, these results are not yet published.

In case of discontinuous load drops (pop-ins) in the force-deflection curve, caused by crack initiation and subsequent crack arrest [21], the procedure for the energy calculation Eq. (1) is modified so that v_m and F_m are replaced by displacement v_{1p} and force F_{1p} of the first significant pop-in (cf. Fig. 2). A load drop is considered as significant, if $\Delta F/F_m \geq 0.1$.

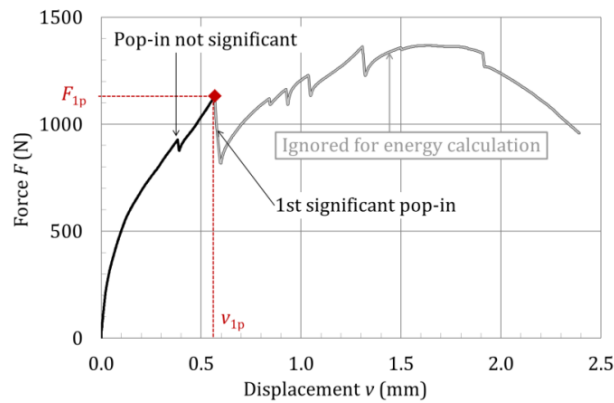


Figure 2. Energy calculation in case of load-drops.

3. Results

3.1. Force-displacement curves

Selected force-displacement curves are shown in Figs. 3-5. For the hot-rolled material ODS-HR, there are significant differences between the orientation L and T on the one hand and orientation S on the other hand. The maximum forces F_m and corresponding displacements v_m are smaller in L/T-oriented samples. Moreover, load-drops (pop-ins) are observed at low test temperatures (below $-70\text{ }^\circ\text{C}$) for orientation L/T but not for orientation S. For room temperature, the parameters v_m and F_m are summarized in Table 2.

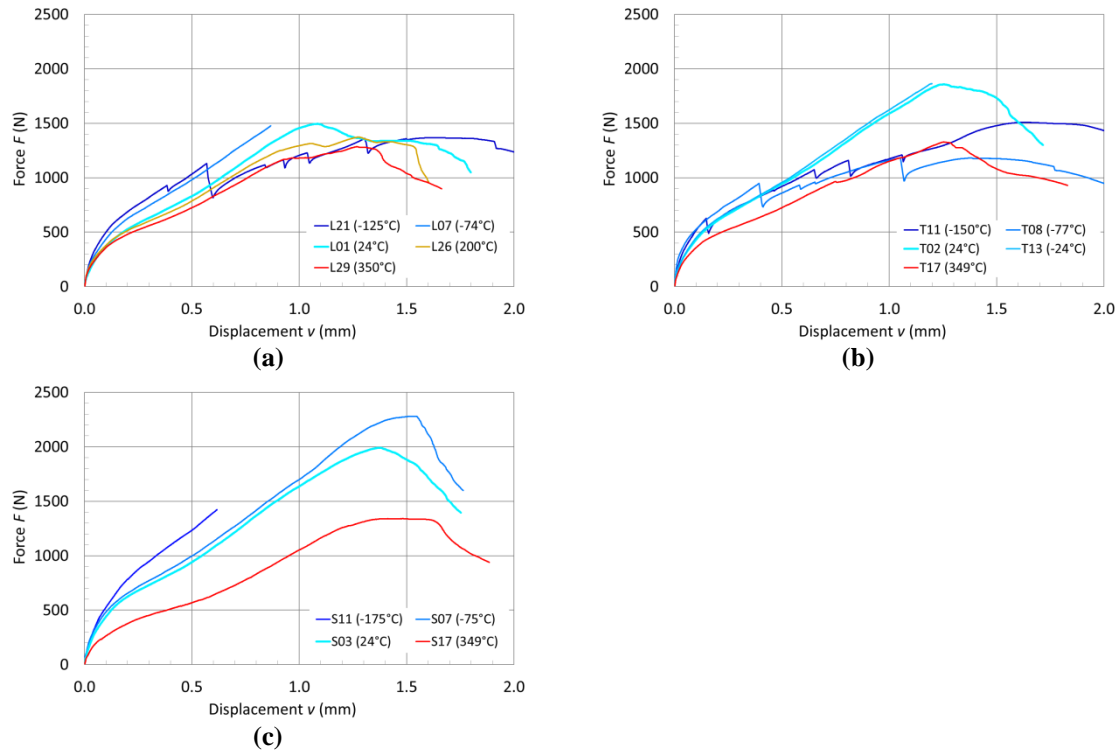


Figure 3. Force-displacement for material ODS-HR; (a) orientation L, (b) orientation T, (c) orientation S.

For the hot extruded materials, pop-ins do not occur in either orientation. The maximum forces F_m and corresponding displacements v_m are slightly smaller in C/R oriented samples as compared to orientation L. There is, however, a pronounced difference between the two materials ODS-HE-01 and ODS-HE-2 in that the latter one exhibits significantly lower absolute values.

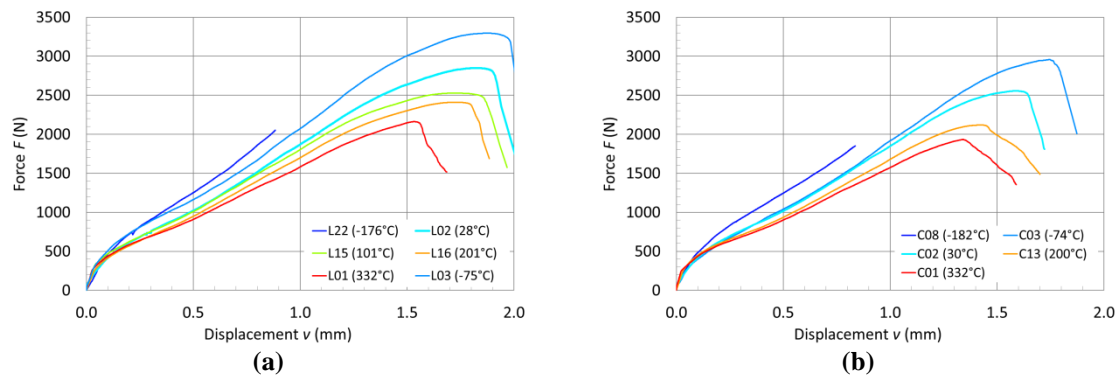


Figure 4. Force-displacement for material ODS-HE-1; (a) orientation L, (b) orientation C/R.

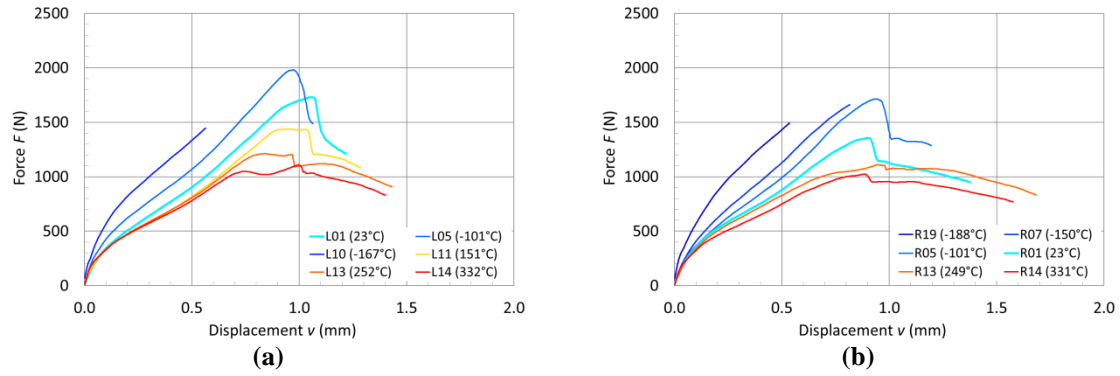


Figure 5. Force-displacement for material ODS-HE-2; (a) orientation L, (b) orientation C/R.

Table 2. Parameters of the force-displacement curves at room temperature.

Material Orientation	ODS-HR L	ODS-HR T	ODS-HR S	ODS-HE-1 L	ODS-HE-1 C/R	ODS-HE-2 L	ODS-HE-2 C/R
v_m (mm)	1.08	1.26	1.37	1.82	1.59	1.05	0.90
F_m (N)	1494	1857	1991	2848	2556	1730	1355

3.2 Ductile-to-brittle transition temperatures

The SP ductile-to-brittle transition temperature were determined for all materials and orientations as described in section 2. Two examples of the dependence of the normalized SP energy E_n on temperature are shown in Fig. 6. The full set of SP transition temperatures T_{SP} and the corresponding recalculated Charpy transition temperature T_{CVN} are given in Table 3.

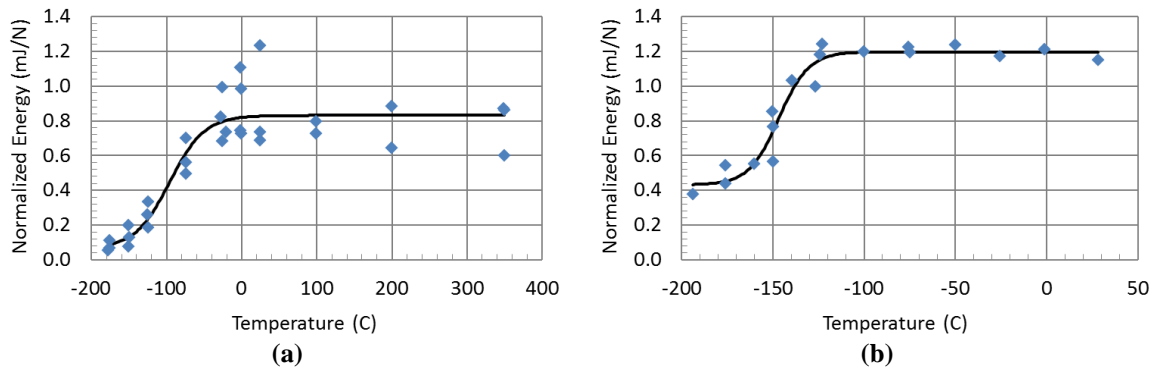


Figure 6. Example of $E_n(T)$ fit curves: (a) ODS-HR orientation L, $T_{SP} = -96$ °C; (b) ODS-HE-1 orientation L, $T_{SP} = -147$ °C.

Table 3. Ductile-to-brittle transitions temperatures.

Material Orientation	ODS-HR L	ODS-HR T	ODS-HR S	ODS-HE-1 L	ODS-HE-1 C/R	ODS-HE-2 L	ODS-HE-2 C/R
T_{SP} (°C)	-96	-70	-157	-147	-130	-144	-154
T_{CVN} (°C) *	+139	+199	-2	+21	+59	+26	+4

* Recalculated from: $T_{SP}[K] = 0.43 \cdot T_{CVN}[K]$

4. Discussion

The microstructure of the investigated ODS steels is characterized by fine and coarse grained regions. In the hot-rolled material ODS-HR the coarse grained regions exhibit elongated pan-cake shaped grains [9] (cf. Fig. 7a), whereas cigar shaped elongated grains were observed in the hot extruded materials ODS-HE-1 and ODS-HE-2 [10] (cf. Fig. 7b).

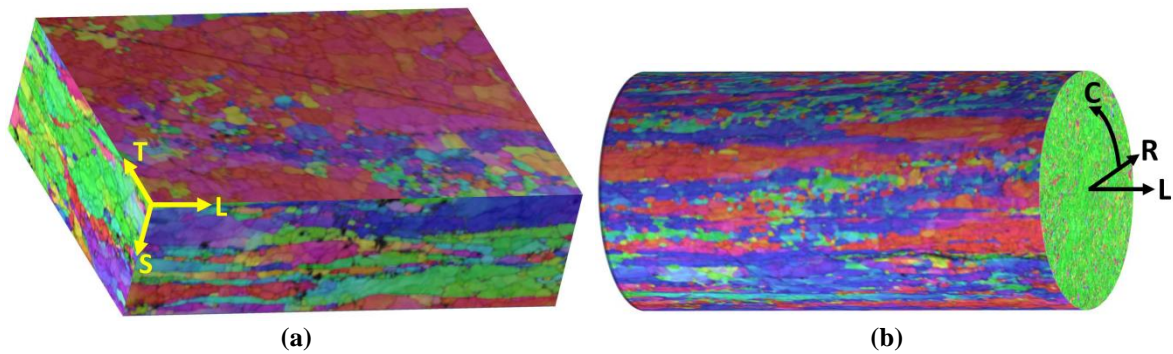


Figure 7. EBSD images from [9,10]: (a) pan-cake shaped coarse grains in ODS-HR; (b) Cigar shaped coarse grains in ODS-HE-1.

It was reported that in the hot rolled material crack extension is preferred through fine grained regions or through the interface between fine grained and coarse grained regions [9]. The large area grain boundaries and the interfaces between coarse and fine grained regions constitute weak interfaces leading to delamination under tensile stress [9,21]. This is the reason why pop-ins are observed in the $F(v)$ curves of L and T oriented samples. The fracture process is characterized by an interplay of stable transgranular crack growth and unstable intergranular crack. Crack arrest occurs when the crack tip arrives at a coarse grain which is extended perpendicularly to the crack propagation direction. The fracture in the SP specimen is preferentially oriented in radial direction and the fracture surface exhibits lamella (cf. Fig 8a). Their formation can be associated with the pop-ins in the $F(v)$ curves. By contrast, such a mechanism does not exist in S oriented samples as the weak interfaces are not loaded by tensile stress. Therefore the crack appearance is the same as for ductile isotropic materials (cf. Fig. 8b).

In hot-extruded materials, the coarse grains are extended only in one direction (L). Thus the SP samples are less susceptible to unstable intergranular cracking and subsequent crack arrest for pure geometrical reasons. Consequently pop-ins cannot be observed in the $F(v)$ curves.

In fracture mechanics investigations by means of 0.25C(T) compact tension samples it was found that the ODS-HR material is susceptible to secondary cracking, i.e. cracks in planes perpendicular to main crack plane were observed [9]. By contrast, the hot-extruded materials ODS-HE-1 and ODS-HE-2 were found to be unsusceptible to secondary cracking [10]. Obviously the occurrence of pop-ins in the SP $F(v)$ curves corresponds with the occurrence of secondary cracks in fracture mechanics testing.

The large differences between ODS-HE-1 and ODS-HE-2 with respect to the v_m and F_m parameters (Table 2) correspond to the different values of fracture toughness reported in [10]. A detailed comparison is given in Table 4.

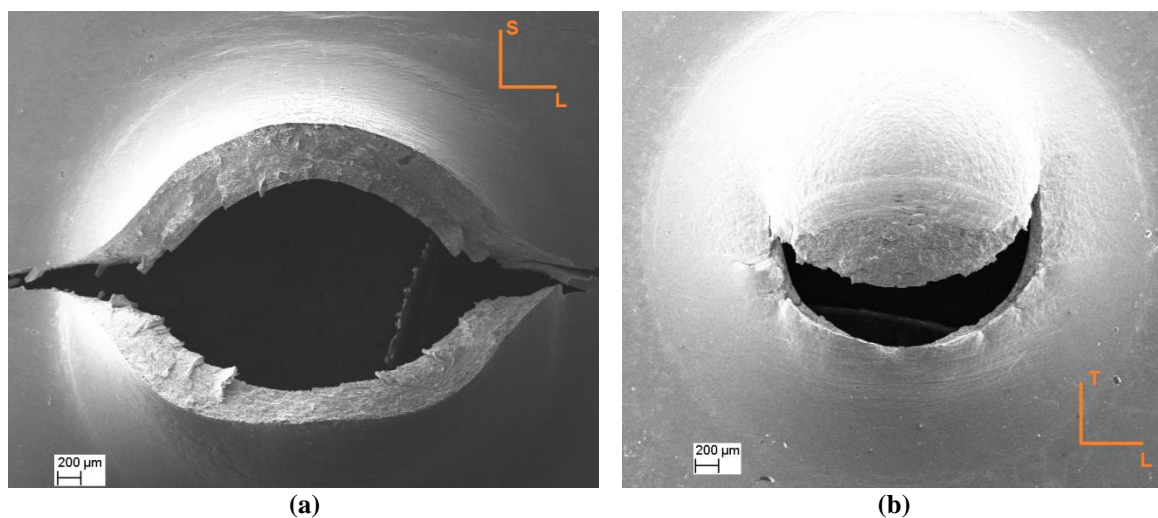


Figure 8. SEM pictures of the fracture modes of samples from ODS-HR: (a) orientation T; (b) orientation S.

Table 4. SP parameters and fracture toughness (from [10]) at room temperature for the hot-extruded materials.

Parameter Orientation	v_m (mm)	F_m (N)	v_m (mm)	F_m (N)	J_Q (kJ/m ²)	J_Q (kJ/m ²)
	L	L	C/R	C/R	L-C	C-R
ODS-HE-1	1.82	2848	1.59	2556	486	97
ODS-HE-2	1.05	1730	0.90	1355	64	35

The existence of coarse Si-rich particles in ODS-HE-2 was identified as main reason for the significantly lower fracture toughness values as compared to ODS-HE-1 [10], also cf. Si content in Table 1. Obviously, the higher values of v_m and F_m in the SP test correspond with higher fracture toughness values J_Q in fracture mechanics testing.

The ductile-to brittle transition temperatures T_{CVN} recalculated from T_{SP} gives reasonable values for the hot-extruded materials (all orientations) and for the hot-rolled material tested with S oriented samples, cf. e.g. [4,21]. The DBTT values between 0 and 60 °C were also found in classical Charpy impact tests and KLST impact tests. In contrast the tests with samples from ODS-HR in orientations L and T give unrealistic high DBTTs. In conclusion, it is suggested that the correlation $T_{SP} = \alpha T_{CVN}$ can be applied for SP tests without pop-ins in the $F(v)$ curves.

5. Conclusions

- In hot-rolled ODS steel, the occurrence of pop-ins in the SP $F(v)$ curves corresponds with the susceptibility to secondary cracks in fracture mechanics testing.
- In hot-extruded ODS steel, higher values of F_m and v_m in the SP test correspond with higher fracture toughness values J_Q in fracture mechanics testing.
- The application of the established correlation between DBTTs from SP test and Charpy impact test ($T_{SP} = \alpha T_{CVN}$) is questionable for L/T oriented SP specimens of hot-rolled ODS material.

Acknowledgments: This work contributes to the Joint Programme on Nuclear Materials (JPNM) of the European Energy Research Alliance (EERA). The cession of two ODS materials by Jan Hoffmann (KIT) is gratefully acknowledged.

References

1. Lindau, R.; Möslang, A.; Rieth, M.; Klimiankou, M.; Materna-Morris, E.; Alamo, A.; Tavassoli, A.-A.F.; Cayron, C.; Lancha, A.-M.; Fernandez, P.; Baluc, N.; Schäublin, R.; Diegele, E.; Filacchioni, G.; Rensman, J.W.; v. d. Schaaf, B.; Lucon, E.; Dietz, W. Present development status of EUROFER and ODS-EUROFER for application in blanket concepts, *Fusion Eng. Des.* 75–79 (2005) 989–996. doi:10.1016/j.fusengdes.2005.06.186.
2. Klueh, R.L.; Shingledecker, J.P.; Swindeman, R.W.; Hoelzer, D.T. Oxide dispersion-strengthened steels: A comparison of some commercial and experimental alloys, *J. Nucl. Mater.* 341 (2005) 103–114. doi:10.1016/j.jnucmat.2005.01.017.
3. McClintock, D.A.; Sokolov, M.A.; Hoelzer, D.T.; Nanstad, R.K. Mechanical properties of irradiated ODS-EUROFER and nanocluster strengthened 14YWT, *J. Nucl. Mater.* 392 (2009) 353–359. doi:10.1016/j.jnucmat.2009.03.024.
4. Lindau, R.; Möslang, A.; Schirra, M.; Schlossmacher, P.; Klimenkov, M. Mechanical and microstructural properties of a hiped RAFM ODS-steel, *J. Nucl. Mater.* 307–311, Part 1 (2002) 769–772. doi:10.1016/S0022-3115(02)01045-0.
5. Chaouadi, R.; Coen, G.; Lucon, E.; Massaut, V. Crack resistance behavior of ODS and standard 9%Cr-containing steels at high temperature, *J. Nucl. Mater.* 403 (2010) 15–18. doi:10.1016/j.jnucmat.2010.05.021.
6. Byun, T.S.; Yoon, J.H.; Wee, S.H.; Hoelzer, D.T.; Maloy, S.A. Fracture behavior of 9Cr nanostructured ferritic alloy with improved fracture toughness, *J. Nucl. Mater.* 449 (2014) 39–48. doi:10.1016/j.jnucmat.2014.03.007.
7. Chao, J.; Capdevila, C.; Serrano, M.; Garcia-Junceda, A.; Jimenez, J.A.; Pimentel, G.; Urones-Garrote, E. Notch Impact Behavior of Oxide-Dispersion-Strengthened (ODS) Fe20Cr5Al Alloy, *Metall. Mater. Trans. A.* 44 (2013) 4581–4594. doi:10.1007/s11661-013-1815-7.

8. Kimura, Y.; Inoue, T.; Yin, F.; Tsuzaki, K. Delamination Toughening of Ultrafine Grain Structure Steels Processed through Tempforming at Elevated Temperatures, *ISIJ Int.* 50 (2010) 152–161. doi:10.2355/isijinternational.50.152.
9. Das, A.; Viehrig, H.W.; Bergner, F.; Heintze, C.; Altstadt, E.; Hoffmann, J. Effect of microstructural anisotropy on fracture toughness of hot rolled 13Cr ODS steel – The role of primary and secondary cracking, *J. Nucl. Mater.* 491 (2017) 83–93. doi:10.1016/j.jnucmat.2017.04.059.
10. Das, A.; Viehrig, H.W.; Altstadt, E.; Heintze, C.; Hoffmann, J. On the influence of microstructure on the fracture behaviour of hot extruded ferritic ODS steels, *J. Nucl. Mater.* 497 (2017) 60–75. doi:10.1016/j.jnucmat.2017.10.051.
11. Misawa, T.; Adachi, T.; Saito, M.; Hamaguchi, Y. Small punch tests for evaluating ductile-brittle transition behavior of irradiated ferritic steels, *J. Nucl. Mater.* 150 (1987) 194–202. doi:10.1016/0022-3115(87)90075-4.
12. Mao, X.; Takahashi, H. Development of a further-miniaturized specimen of 3 mm diameter for tem disk (\varnothing 3 mm) small punch tests, *J. Nucl. Mater.* 150 (1987) 42–52. doi:10.1016/0022-3115(87)90092-4.
13. Jia, X.; Dai, Y. Small punch tests on martensitic/ferritic steels F82H, T91 and Optimax-A irradiated in SINQ Target-3, *J. Nucl. Mater.* 323 (2003) 360–367. doi:10.1016/j.jnucmat.2003.08.018.
14. Fleury, E.; Ha, J.S. Small punch tests to estimate the mechanical properties of steels for steam power plant: I. Mechanical strength, *Int. J. Press. Vessels Pip.* 75 (1998) 699–706. doi:10.1016/S0308-0161(98)00074-X.
15. Kameda, J.; Mao, X. Small-punch and TEM-disc testing techniques and their application to characterization of radiation damage, *J. Mater. Sci.* 27 (1992) 983–989. doi:10.1007/BF01197651.
16. Dymáček, P.; Milička, K. Creep small-punch testing and its numerical simulations, *Mater. Sci. Eng. A.* 510–511 (2009) 444–449. doi:10.1016/j.msea.2008.06.053.
17. Altstadt, E.; Ge H.E.; Kuksenko, V.; Serrano, M.; Houska, M.; Lasan, M.; Bruchhausen, M.; Lapetite, J.-M.; Dai, Y. Critical evaluation of the small punch test as a screening procedure for mechanical properties, *J. Nucl. Mater.* 472 (2016) 186–195. doi:10.1016/j.jnucmat.2015.07.029.
18. Altstadt, E.; Houska, M.; Simonovski, I.; Bruchhausen, M.; Holmström, S.; Lacalle, R. On the estimation of ultimate tensile stress from small punch testing, *Int. J. Mech. Sci.* 136 (2018) 85–93. doi:10.1016/j.ijmecsci.2017.12.016.
19. Vivas, J.; Capdevila, C.; Altstadt, E.; Houska, M.; San-Martín, D. Importance of austenitization temperature and ausforming on creep strength in 9Cr ferritic/martensitic steel, *Scr. Mater.* 153 (2018) 14–18. doi:10.1016/j.scriptamat.2018.04.038.
20. Okuda, N.; Kasada, R.; Kimura, A. Statistical evaluation of anisotropic fracture behavior of ODS ferritic steels by using small punch tests, *J. Nucl. Mater.* 386–388 (2009) 974–978. doi:10.1016/j.jnucmat.2008.12.265.
21. Altstadt, E.; Serrano, M.; Houska, M.; García-Junceda, A. Effect of anisotropic microstructure of a 12Cr-ODS steel on the fracture behaviour in the small punch test, *Mater. Sci. Eng. A.* 654 (2016) 309–316. doi:10.1016/j.msea.2015.12.055.
22. Hoffmann, J.; Rieth, M.; Commin, L.; Antusch, S. Microstructural anisotropy of ferritic ODS alloys after different production routes, *Fusion Eng. Des.* 98–99 (2015) 1986–1990. doi:10.1016/j.fusengdes.2015.05.002.
23. Bruchhausen, M.; Austin, T.; Holmström, S.; Altstadt, E.; Dymacek, P.; Jeffs, S.; Lancaster, R.; Lacalle, R.; Matocha, K.; Petzová, J. European Standard on Small Punch Testing of Metallic Materials, in: ASME, 2017: p. V01AT01A065. doi:10.1115/PVP2017-65396.
24. Bruchhausen, M.; Holmström, S.; Lapetite, J.-M.; Ripplinger, S. On the determination of the ductile to brittle transition temperature from small punch tests on Grade 91 ferritic-martensitic steel, *Int. J. Press. Vessels Pip.* 155 (2017) 27–34. doi:10.1016/j.ijpvp.2017.06.008.